

## Research Article

# Comparative Study of SiO<sub>2</sub>, Al<sub>2</sub>O<sub>3</sub>, and BeO Ultrathin Interfacial Barrier Layers in Si Metal-Oxide-Semiconductor Devices

J. H. Yum,<sup>1,2</sup> J. Oh,<sup>3</sup> Todd. W. Hudnall,<sup>4</sup> C. W. Bielawski,<sup>5</sup>  
G. Bersuker,<sup>2</sup> and S. K. Banerjee<sup>1</sup>

<sup>1</sup>Microelectronics Research Center, Department of Electrical and Computer Engineering, The University of Texas, Austin, TX 78758, USA

<sup>2</sup>SEMATECH, 2706 Montopolis Drive, Austin, TX 78741, USA

<sup>3</sup>School of Integrated Technology, College of Engineering, Yonsei University, 162-1 Songdo-dong, Incheon 406-840, Republic of Korea

<sup>4</sup>Department of Chemistry and Biochemistry, Texas State University, 601 University Drive, San Marcos, TX 78666, USA

<sup>5</sup>Department of Chemistry, UT, Austin, TX 78712, USA

Correspondence should be addressed to J. H. Yum, redehyes78@mail.utexas.edu

Received 19 March 2012; Accepted 12 September 2012

Academic Editor: Edward Yi Chang

Copyright © 2012 J. H. Yum et al. This is an open access article distributed under the Creative Commons Attribution License, which permits unrestricted use, distribution, and reproduction in any medium, provided the original work is properly cited.

In a previous study, we have demonstrated that beryllium oxide (BeO) film grown by atomic layer deposition (ALD) on Si and III-V MOS devices has excellent electrical and physical characteristics. In this paper, we compare the electrical characteristics of inserting an ultrathin interfacial barrier layer such as SiO<sub>2</sub>, Al<sub>2</sub>O<sub>3</sub>, or BeO between the HfO<sub>2</sub> gate dielectric and Si substrate in metal oxide semiconductor capacitors (MOSCAPs) and n-channel inversion type metal oxide semiconductor field effect transistors (MOSFETs). Si MOSCAPs and MOSFETs with a BeO/HfO<sub>2</sub> gate stack exhibited high performance and reliability characteristics, including a 34% improvement in drive current, slightly better reduction in subthreshold swing, 42% increase in effective electron mobility at an electric field of 1 MV/cm, slightly low equivalent oxide thickness, less stress-induced flat-band voltage shift, less stress induced leakage current, and less interface charge.

## 1. Introduction

The CMOS scaling is bringing the SiO<sub>2</sub> thickness below 1.5 nm. For these very thin oxides, the leakage current becomes unacceptably large. One way to reduce the leakage current is the substitution of the SiO<sub>2</sub> by a material with a higher dielectric constant. The main advantage of high-k dielectrics is the low gate leakage achieved due to its high physical thickness. That also makes it attractive for low power applications. Because of these requirements, over the past 10 years, hafnium oxide (HfO<sub>2</sub>) has gained considerable interest as a high dielectric constant material for fabricating complementary metal oxide semiconductor (CMOS) devices. It has several attractive properties such as a high dielectric constant, good thermodynamic stability with Si, and good electrical properties [1]. Unfortunately, some of the other physical properties like mobility reduction, charge

trapping, and threshold voltage ( $V_{th}$ ) instability are a major drawback for the performance of metal oxide semiconductor field effect transistors (MOSFETs) [2]. Especially HfO<sub>2</sub> high-k dielectric stacked MOSFETs were reported with low carrier mobility [3]. The main cause for the low mobility is still unknown, but has been attributed to remote Coulomb scattering caused by charges in the high-k dielectric [4] or optical phonon scattering [5]. Many researchers have believed that it is inevitable for all high-k dielectrics to have low energy bandgap and high scattering, compared to SiO<sub>2</sub>. Therefore, if high-k dielectric with high energy bandgap and low scattering can be found, it will be the true solution for the above problems.

An alternative promising high-k gate dielectric material is beryllium oxide (BeO), which has superior interface stability [6–10] and is already known as an excellent gas diffusion barrier. This makes it a potentially suitable diffusion barrier

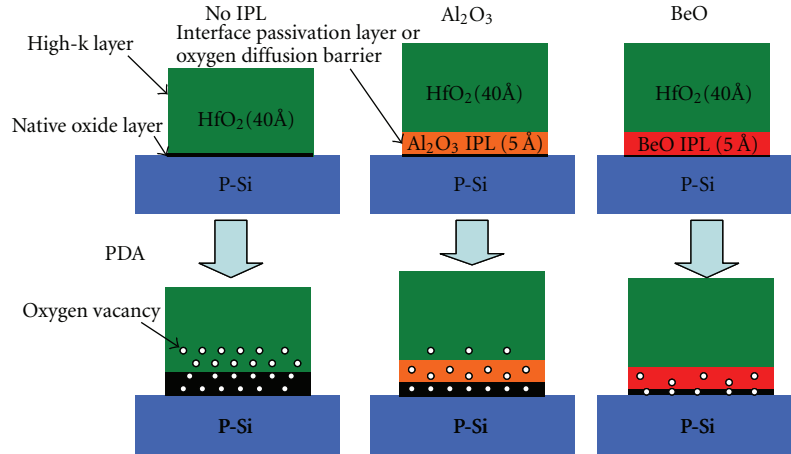


FIGURE 1: Cross-sectional MOS devices with various IL. The BeO interfacial layer is placed between HfO<sub>2</sub> and p-type Si substrate.

between HfO<sub>2</sub> and Si in CMOS processing. BeO also has metal-like thermal conductivity and a large energy bandgap (10.6 eV). These properties are indicative of low optical phonon and remote Coulomb scattering. Generally, a flow of phonons is responsible for heat conduction in dielectric materials. As the temperature increases, phonon density increases, but above 20 K, the phonon-phonon interaction becomes dominant and reduces the mean free path of the phonon drift, degrading thermal conductivity in the dielectrics [11]. BeO, however, has high thermal conductivity due to low phonon scattering because electrons in BeO are tightly and closely bound, so that the phonons in BeO are coupled to each other and have low energy and long wavelengths (or low phonon frequency). The high energy bandgap and band offset of BeO on Si makes intrinsic charge trapping difficult and results in a low trapped charge in the BeO dielectric (trapped charges in high-k dielectrics are the source of Coulomb scattering) [10]. Our previous studies have showed electrical and physical characteristics that BeO deposited with dimethylberyllium and water improves interface quality on III-V MOS devices by preventing sub-oxidation between high-k and III-V substrate during PDA [6]. In this paper, we compare the effect of interfacial barrier layer by inserting ultrathin SiO<sub>2</sub>, Al<sub>2</sub>O<sub>3</sub>, or BeO barrier layer (IL) between the HfO<sub>2</sub> gate dielectric and Si substrate in metal oxide semiconductor capacitors (MOSCAPs) and NMOSFETs. The aim of using such a barrier layer was to improve the device performance and reliability while maintaining, as much as possible, the overall dielectric constant of the resulting film.

## 2. Fabrication Procedure

An ALD BeO IL was deposited on HF-last p-type Si substrates using dimethylberyllium precursors and water as an oxygen source. As a reference, ALD Al<sub>2</sub>O<sub>3</sub> IL was deposited on the same cleaned substrate using trimethylaluminum and the same oxygen source. Samples with a BeO IL, Al<sub>2</sub>O<sub>3</sub> IL, and without an IL were followed by ALD HfO<sub>2</sub>. They were annealed for 3 min at 600°C in N<sub>2</sub>

at atmospheric pressure. The physical thickness of the BeO and Al<sub>2</sub>O<sub>3</sub> IL layers was controlled from the deposition rate which was measured on the bulk oxide using multiple-wavelength (200~900 nm) ellipsometry. The TaN electrode was deposited using reactive dc magnetron sputtering at 2000 Å followed by reactive ion etching (RIE) with Ar + CF<sub>4</sub> after electrode patterning of the gate. The source/drain (S/D) regions of NMOSFETs were implanted with phosphorus at 50 keV and a dose of  $5 \times 10^{15} \text{ cm}^{-2}$ . High temperature (900°C, 1 min) annealing in N<sub>2</sub> ambient was used for S/D activation. E-beam evaporated Ni/AuGe/Au was used for both S/D and backside metallization. The final sintering was done at 400°C in forming gas for 30 min. For all MOSCAPs samples, PMA (500°C, 2 min) was done.

## 3. Results and Discussion

Figure 1 shows the cross-sectional MOS structure with various IL (or IPL). It is constructed based on the electrical and physical results in the previous experiments [10]. SiO<sub>2</sub>, Al<sub>2</sub>O<sub>3</sub>, or BeO IL is placed between HfO<sub>2</sub> and the P-Si substrate. Al<sub>2</sub>O<sub>3</sub> and BeO IL are intentionally inserted, but SiO<sub>2</sub> IL is thermally grown during post-deposition and S/D activation anneals. In Figure 2, the BeO(IL)/HfO<sub>2</sub> structures show the lowest leakage, comparable to those of SiO<sub>2</sub>(IL)/HfO<sub>2</sub> and Al<sub>2</sub>O<sub>3</sub>(IL)/HfO<sub>2</sub> gate stacks. Insertion of BeO IL (5~10 Å) doesn't increase the EOT significantly after the post-deposition anneal (PDA) due to the efficient suppression of the oxygen diffusion during PDA. The effectiveness of oxygen diffusion barrier for BeO IL is more presented as the annealing temperature increases in Figure 3. BeO IL may have some advantage for EOT scaling and reliability improvement After S/D activation, around 15 Å SiO<sub>2</sub> is grown at the interface between HfO<sub>2</sub> and the Si substrate. The low EOT of BeO IL is an indication of efficient oxygen diffusion barrier. The similar results were presented using X-ray photoelectron spectroscopy (XPS) [10]. Oxygen diffusion through thin films is proportional to the number and size of pinholes in the respective film [12]. In general, smaller pinholes cause more collisions between the diffusing

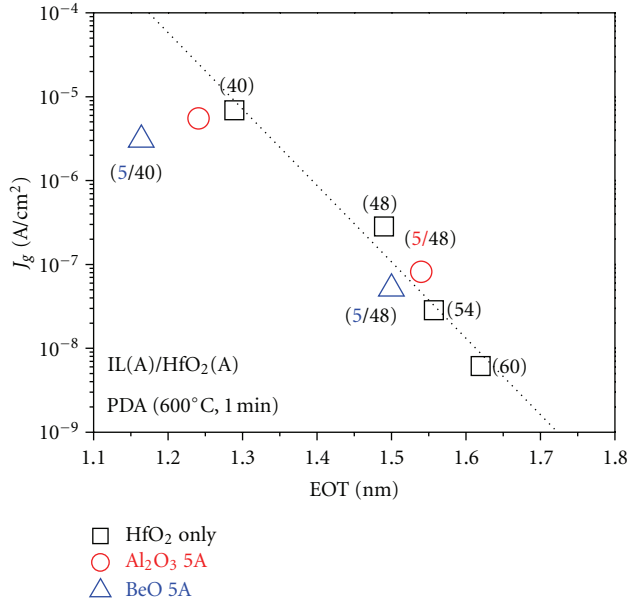


FIGURE 2: Gate leakage current versus EOT for SiO<sub>2</sub>/HfO<sub>2</sub>, Al<sub>2</sub>O<sub>3</sub>(IL)/HfO<sub>2</sub>, and BeO(IL)/HfO<sub>2</sub> gate stacks.

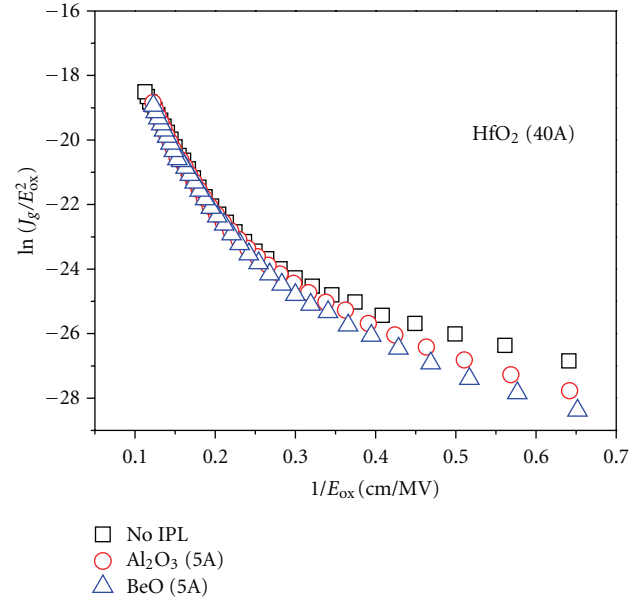


FIGURE 4: F-N plots to compare the effective potential barrier height for three different gate stacks.

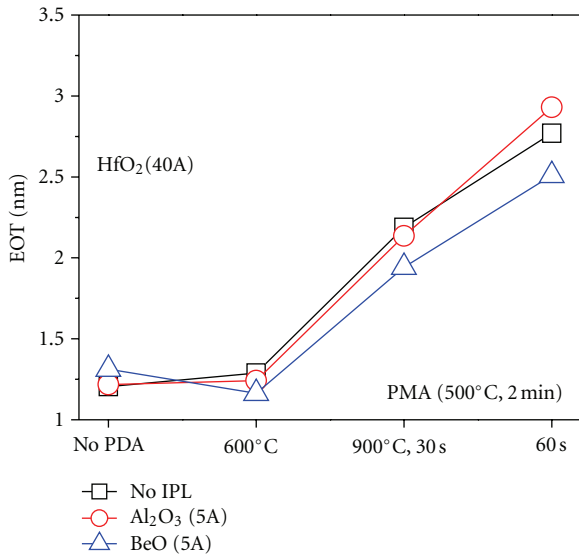


FIGURE 3: The change of EOT with the annealing temperature and duration for three different gate stacks.

molecules (e.g., oxygen) and the chemical groups present in the bulk film, reducing the rate of permeation. For reasons that are still under investigation, films of BeO, which have small molecular size, appear to exhibit relatively low oxygen diffusivity and are capable of effectively blocking the diffusion of impurities, such as Hf, thus minimizing defects in the substrate.

In general, the bandgap of the high- $k$  material is inversely proportional to its permittivity, but BeO is an exception, having a very large energy bandgap (10.6 eV) combined with a still high dielectric constant of 6.8. As the bandgap, or

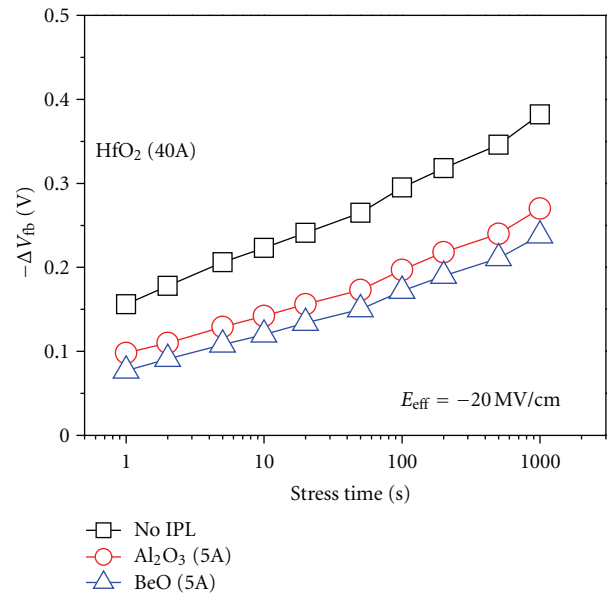


FIGURE 5: Stress-induced  $V_{fb}$  shift ( $\Delta V_{fb}$ ) versus stress time for three different gate stacks.  $E_{eff} = (V_g - V_{fb})/EOT$ .

correspondingly, band offset increases, a charge trapping in the dielectric decreases. The effective potential barrier heights for SiO<sub>2</sub>/HfO<sub>2</sub>, Al<sub>2</sub>O<sub>3</sub>(IL)/HfO<sub>2</sub>, and BeO(IL)/HfO<sub>2</sub> gate stacks are compared using the Fowler-Nordheim plot in Figure 4. Due to bilayer gate structure, exact number of the effective barrier height is not extracted. But a higher barrier of the BeO IL stack is observed and it may results in the smaller electron tunneling currents, compared to other different gate stacks. Figures 5 and 6 are the representative results of reliability statistics characteristics. In Figure 5,

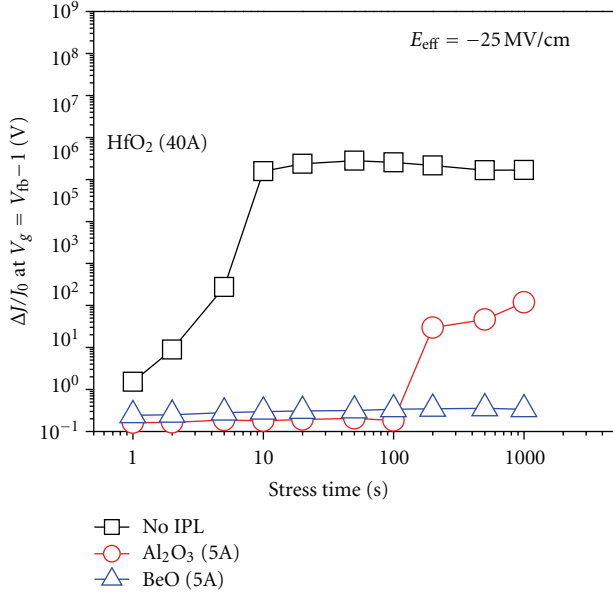


FIGURE 6: Stress-induced leakage current ( $\Delta J_g/J_0$ ) versus stress time.  $E_{\text{eff}} = (V_g - V_{\text{fb}})/\text{EOT}$ .

the BeO(IL)/HfO<sub>2</sub> gate stack shows less initial  $V_{\text{fb}}$  shift (after 1 sec stress) indicating fewer preexisting traps in the dielectric. A slightly smaller trap generation rate was also observed compared to other two gate stacks. In Figure 6, the BeO(IPL)/HfO<sub>2</sub> also shows the reduced stress-induced leakage current (SILC) degradation and no significant breakdown. But SiO<sub>2</sub>/HfO<sub>2</sub> and Al<sub>2</sub>O<sub>3</sub>(IL)/HfO<sub>2</sub> show gradual breakdown with stress time. The lower trap generation rate and the reduced tunneling current of the BeO(IPL)/HfO<sub>2</sub> gate stack may improve the reliability characteristics and it may be the indication of the high structural stability. In the view point of thermodynamics of materials, the total entropy of a material consists of its thermal entropy, which is related to thermal conductivity, and configurational entropy, which is related to the crystallization (or crystallinity) of the material [13]. With high crystallinity and thermal conductivity, BeO may have high total entropy, and it means that BeO is more structurally stable, compared to other gate dielectrics, even though the direct correlation between thermodynamic stability and device performance is still questionable. For more details of BeO thermal stability, please see the reference [14]

Figure 7 is NMOSFET inversion capacitance for SiO<sub>2</sub>/HfO<sub>2</sub> (40 Å), Al<sub>2</sub>O<sub>3</sub>(5 Å)/HfO<sub>2</sub> (40 Å), and BeO(5 Å)/HfO<sub>2</sub> (40 Å) gate stacks. The BeO/HfO<sub>2</sub> gate stack shows a slightly lower equivalent oxide thickness (EOT) (2.51 nm) than SiO<sub>2</sub>/HfO<sub>2</sub> (2.77 nm) and Al<sub>2</sub>O<sub>3</sub>/HfO<sub>2</sub> (2.93 nm) even though the EOTs for all gate stacks significantly increased after S/D activation annealing (Figure 3). From the XPS analysis, EOT increase is mainly due to the oxygen in HfO<sub>2</sub> dielectric, instead of oxygen residue in anneal tool [10]. For SiO<sub>2</sub>/HfO<sub>2</sub>, Al<sub>2</sub>O<sub>3</sub>/HfO<sub>2</sub>, and BeO/HfO<sub>2</sub> gate stacks, 1.7 nm, 1.5 nm, and 1.0 nm are expected for native oxide to be grown, respectively, based on Figure 3 results. Figure 8

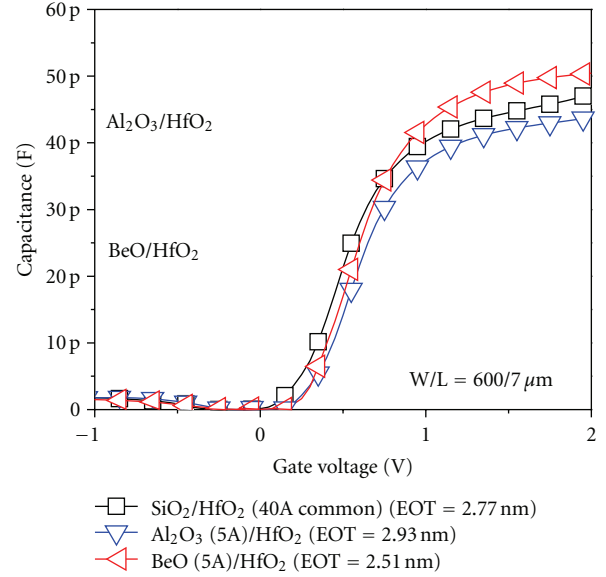


FIGURE 7: NMOSFETs inversion capacitance for three different gate stacks.

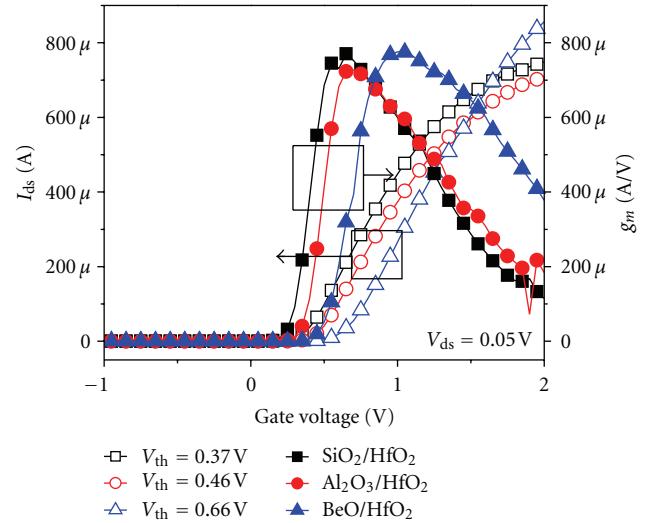


FIGURE 8: NMOSFETs  $I_d - V_g$  characteristics of three gate stacks. BeO IL shows slightly higher  $V_{\text{th}}$ ,  $G_m$ , and  $I_d$ .

shows NMOSFET drain current-gate voltage ( $I_d - V_g$ ) characteristics of SiO<sub>2</sub>/HfO<sub>2</sub>, Al<sub>2</sub>O<sub>3</sub>/HfO<sub>2</sub>, and BeO/HfO<sub>2</sub> gate stacks. With the slightly lower EOT, the BeO/HfO<sub>2</sub> stack exhibits more positive  $V_{\text{th}}$  (0.66 V), higher drive current at  $V_g = 2$  V, and better subthreshold swing (69 mV/dec), compared to those of the SiO<sub>2</sub>/HfO<sub>2</sub> stack ( $V_{\text{th}} = 0.37$  V, SS = 77 mV/dec) and Al<sub>2</sub>O<sub>3</sub>/HfO<sub>2</sub> stack ( $V_{\text{th}} = 0.46$  V, SS = 70 mV/dec). The threshold voltage equation obtained from an ideal MOS structure [15] is

$$V_{\text{th}} = \Phi_{\text{ms}} - \frac{Q_i}{C_i} - \frac{Q_d}{C_i} + 2\phi_F, \quad (1)$$

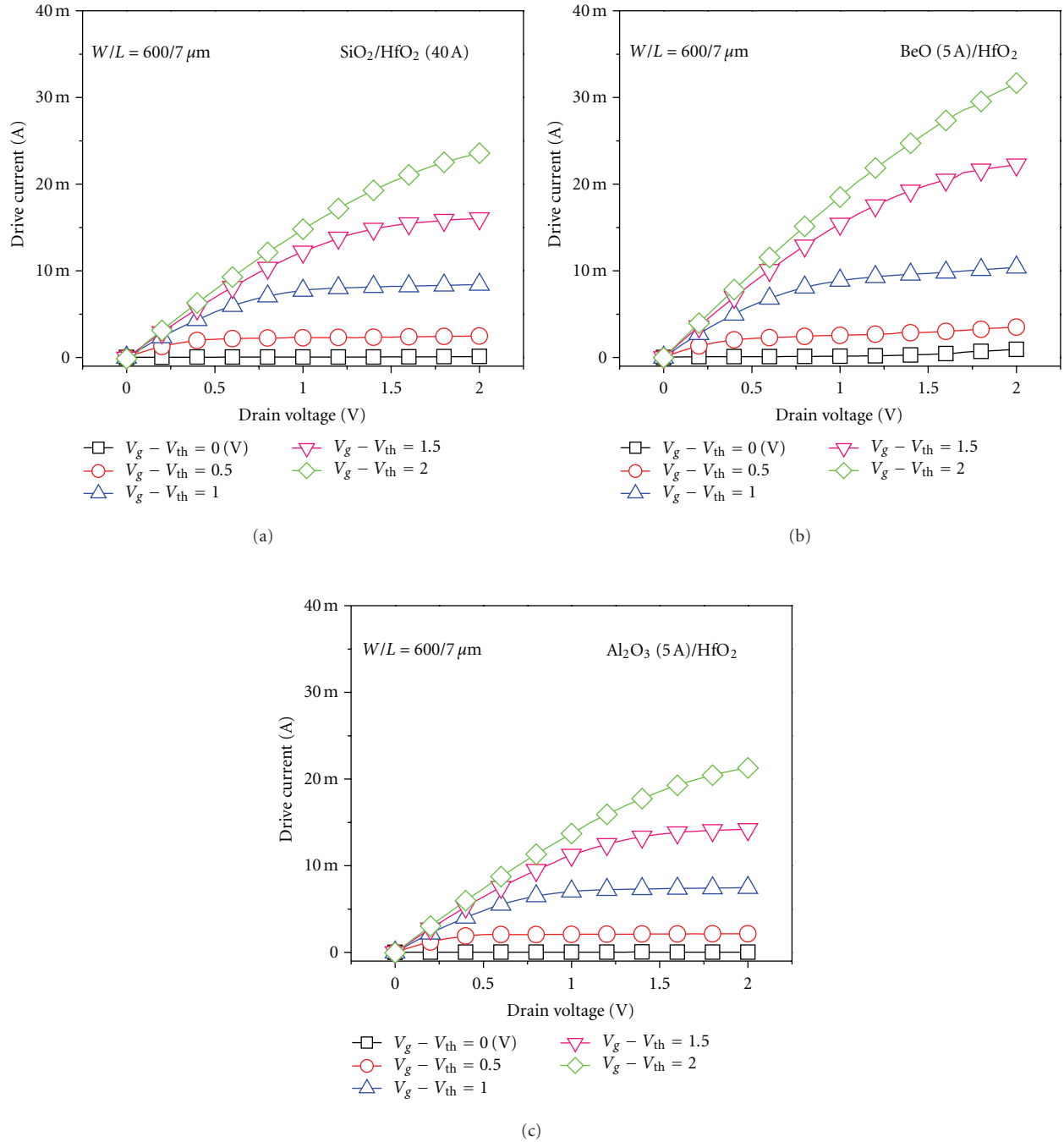


FIGURE 9:  $I_d - V_d$  characteristics of three gate stacks. BeO IL shows significant increased drive current compared to  $\text{SiO}_2$  and  $\text{Al}_2\text{O}_3$  IL gate stacks.

where  $\Phi_{ms}$ ,  $Q_i$ ,  $Q_d$ , and  $\phi_F$  are the work function differences between the metal and semiconductor (“-” value), interface charge (“+” value), depletion charge (“-” value) for the n-channel, and energy differences between the intrinsic energy level and Fermi energy level (+) for the n-channel,  $\phi_F = (E_i - E_F)/q$ . If we assume that  $\Phi_{ms}$ ,  $Q_d$ , and  $\phi_F$  are the same for all gate stacks because the only difference is interfacial layer, then the positive shift of  $V_{th}$  of the BeO/ $\text{HfO}_2$  stack is due to the less positive interface charges between BeO and

the Si substrate. The fewer fixed charges in BeO layer may contribute to the fewer interface charges [10].

In Figure 9, the BeO/ $\text{HfO}_2$  stack shows around 34% higher drive current (31.67 mA) at  $V_d = 2$  V &  $V_g - V_{th} = 2$  V than the  $\text{SiO}_2/\text{HfO}_2$  stack (23.56 mA) and  $\text{Al}_2\text{O}_3/\text{HfO}_2$  stack (21.28 mA). Only 5 Å BeO insertion between high-k and Si channel makes the drive current much improved. There is some reduction of drive current with the IL thickness increase for both the  $\text{Al}_2\text{O}_3/\text{HfO}_2$  and BeO/ $\text{HfO}_2$

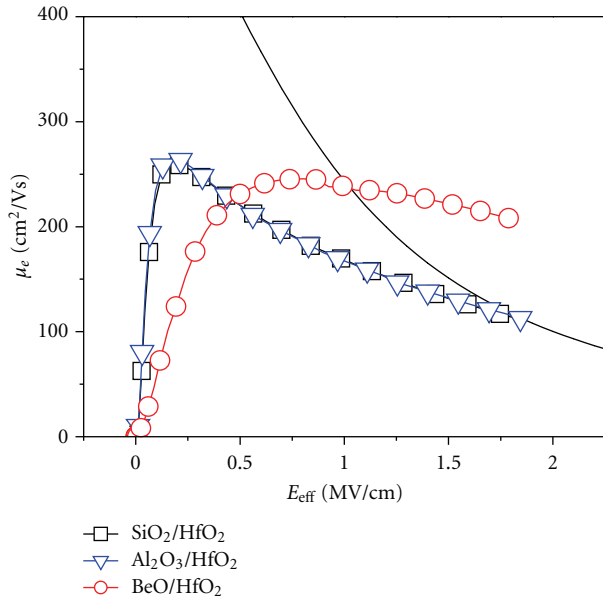


FIGURE 10: Effective channel mobility of NMOSFETs with three gate stacks.

gate stacks, but it is more significant on Al<sub>2</sub>O<sub>3</sub>/HfO<sub>2</sub> stack. It may be due to the less native interfacial oxide (SiO<sub>2</sub>) growth for Al<sub>2</sub>O<sub>3</sub>/HfO<sub>2</sub> stack. Figure 10 illustrates the effective channel electron mobility using the split capacitance-voltage (C-V) method. The BeO/HfO<sub>2</sub> stack shows a 42% higher effective field ( $E_{eff}$ ) mobility (238 cm<sup>2</sup>/Vs) than SiO<sub>2</sub>/HfO<sub>2</sub> (167 cm<sup>2</sup>/Vs) and Al<sub>2</sub>O<sub>3</sub>/HfO<sub>2</sub> (166 cm<sup>2</sup>/Vs) at  $E_{eff} = 1$  MV/cm. It may require further investigation to confirm and explain these results. The electron mobility in SiO<sub>2</sub>/HfO<sub>2</sub> and Al<sub>2</sub>O<sub>3</sub>/HfO<sub>2</sub> are fast-saturated to the universal trend, likely due to the thick SiO<sub>2</sub> interfacial layer grown during S/D activation. If the SiO<sub>2</sub> interfacial layer is thinner, the peak electron mobilities of the HfO<sub>2</sub> gate stack will decrease significantly [16]. In atomic configuration, physical roughness difference between amorphous Al<sub>2</sub>O<sub>3</sub> and crystalline BeO is similar, but in electronic configuration, the electrostatic potential roughness between them is quite different. In terms of electrostatic potential roughness, the two-dimensional ordered arrays of atoms on a crystalline surface generally give atomic scale surface height fluctuation, which exhibits low electrostatic potential roughness [17]. In a previous study, we demonstrated that ALD BeO on Si grows almost epitaxially [7], thereby may improve surface electro-potential roughness and high field electron mobility.

In this work, a BeO (IL)/HfO<sub>2</sub> gate stack was investigated and systematically compared to a SiO<sub>2</sub>/HfO<sub>2</sub> gate stack. Inserting an ALD BeO IL between the Si channel and high-k gate dielectric enhances high field carrier mobility and improves MOSFET parameter and reliability characteristics while maintaining a similar EOT. Excellent BeO properties, such as a high energy bandgap, efficient oxygen diffusion barrier, and high crystallinity, improve the charge trapping, the suppression in EOT increase during S/D activation, and

MOSFET performance, thus imparting significant advantages to MOS devices with a BeO IL.

## Acknowledgments

This work was supported in part by the Robert Welch Foundation (Grants F-1038 and F-1621) and NSF (Grant DMR-0706227).

## References

- [1] K. J. Hubbard and D. G. Schlom, "Thermodynamic stability of binary oxides in contact with silicon," *Journal of Materials Research*, vol. 11, no. 11, pp. 2757–2776, 1996.
- [2] A. Kerber, E. Cartier, R. Degraeve, L. Pantisano, P. Roussel, and G. Groeseneken, "Strong correlation between dielectric reliability and charge trapping in SiO<sub>2</sub>/Al<sub>2</sub>O<sub>3</sub> gate stacks with TiN electrodes," in *Proceedings of the Symposium on VLSI Technology Digest of Technical Papers*, pp. 76–77, June 2002.
- [3] Y. Kim, G. Gebara, M. Freiler et al., "Conventional n-channel MOSFET devices using single layer HfO<sub>2</sub> and ZrO<sub>2</sub> as high-k gate dielectrics with polysilicon gate electrode," in *IEEE International Electron Devices Meeting (IEDM '01)*, pp. 455–458, Washington, DC, USA, December 2001.
- [4] S. Saito, Y. Shimamoto, K. Torii et al., "The mechanism of mobility degradation in MISFETs with Al<sub>2</sub>O<sub>3</sub> gate dielectric," in *Proceedings of the Symposium on VLSI Technology Digest of Technical Papers*, pp. 188–189, June 2002.
- [5] M. V. Fischetti, D. A. Neumayer, and E. A. Cartier, "Effective electron mobility in Si inversion layers in metal-oxide-semiconductor systems with a high- $\kappa$  insulator: the role of remote phonon scattering," *Journal of Applied Physics*, vol. 90, no. 9, pp. 4587–4608, 2001.
- [6] J. H. Yum, T. Akyol, M. Lei et al., "Atomic layer deposited beryllium oxide: effective passivation layer for III-V metal/oxide/semiconductor devices," *Journal of Applied Physics*, vol. 109, no. 6, Article ID 064101, 2011.
- [7] J. H. Yum, T. Akyol, M. Lei et al., "A study of highly crystalline novel beryllium oxide film using atomic layer deposition," *Journal of Crystal Growth*, vol. 334, pp. 126–133, 2011.
- [8] J. H. Yum, T. Akyol, M. Lei et al., "Inversion type InP metal oxide semiconductor field effect transistor using novel atomic layer deposited BeO gate dielectric," *Applied Physics Letters*, vol. 99, no. 3, Article ID 033502, 2011.
- [9] J. H. Yum, T. Akyol, M. Lei et al., "Comparison of the self-cleaning effects and electrical characteristics of BeO and Al<sub>2</sub>O<sub>3</sub> deposited as an interface passivation layer on GaAs MOS devices," *Journal of Vacuum Science and Technology A*, vol. 29, no. 6, Article ID 061501, 2011.
- [10] J. H. Yum, T. Akyol, M. Lei et al., "Epitaxial ALD BeO: efficient oxygen diffusion barrier for EOT scaling and reliability improvement," *Electron Device Letters*, vol. 58, no. 12, pp. 4384–4392, 2011.
- [11] R. E. Hummel, *Electronic Properties of Materials*, chapter 21, 3rd edition, 2001.
- [12] A. A. Dameron, S. D. Davidson, B. B. Burton, P. F. Carcia, R. S. McLean, and S. M. George, "Gas diffusion barriers on polymers using multilayers fabricated by Al<sub>2</sub>O<sub>3</sub> and rapid SiO<sub>2</sub> atomic layer deposition," *Journal of Physical Chemistry C*, vol. 112, no. 12, pp. 4573–4580, 2008.
- [13] D. R. Gaskell, *Introduction to the Thermodynamics of Materials*, chapter 4, 5th edition, 2008.

- [14] J. H. Yum, G. Bersuker, J. Oh, and S. K. Banerjee, "Theoretical approach evaluating beryllium oxide as A gate dielectric in the view points of electromagnetics and thermal stability," *Applied Physics Letters*, vol. 100, no. 5, Article ID 053501, 3 pages, 2012.
- [15] B. G. Streetman and S. K. Banerjee, *Solid State Electronic Devices*, 6th edition, 2005.
- [16] S. J. Rhee, C. Y. Kang, C. S. Kang et al., "Effects of varying interfacial oxide and high-k layer thicknesses for HfO<sub>2</sub> metal-oxide-semiconductor field effect transistor," *Applied Physics Letters*, vol. 85, no. 7, pp. 1286–1288, 2004.
- [17] Y. Zhao, G. C. Wang, and T. M. Lu, *Characterization of Amorphous and Crystalline Rough Surface: Principles and Applications*, chapter 6, 7, and 16, 2000.



**Hindawi**

Submit your manuscripts at  
<http://www.hindawi.com>

